NASA/CP-2000-210291

Fifth International Symposium on Magnetic Suspension Technology

Edited by
Nelson J. Groom
Langley Research Center, Hampton, Virginia

Colin P. Britcher
Old Dominion University, Norfolk, Virginia

Proceedings of a workshop sponsored by the National Aeronautics and Space Administration, Washington, DC; the National Aerospace Laboratory, Tokyo, Japan; and the National High Magnetic Field Laboratory, Tallahassee, Florida and held in Santa Barbara, California December 1-3, 1999

National Aeronautics and Space Administration

Langley Research Center
Hampton, Virginia 23681-2199

July 2000

Available from:

NASA Center for AeroSpace Information (CASI)
7121 Standard Drive
Hanover, MD 21076-1320
(301) 621-0390

National Technical Information Service (NTIS)
5285 Port Royal Road
Springfield, VA 22161-2171
(703) 605-6000

INTRODUCTION

The Fifth International Symposium on Magnetic Suspension Technology was held at the Radisson Hotel Santa Barbara in Santa Barbara, California, on December 1-3, 1999. The Symposium was sponsored by the Guidance and Control Branch of the Langley Research Center, in coordination with NASA Headquarters, the National Aerospace Laboratory (NAL), Japan, and the National High Magnetic Field Laboratory (NHMFL) operated by Florida State University. The symposium was hosted by the University of California at Santa Barbara (UCSB) Center for Control Engineering and Computation.

The organizing committee and symposium committee consisted of the following people:

ORGANIZING COMMITTEE

Nelson J. Groom, Chair
NASA Langley Research Center
Hampton, VA 23681-2199
U.S.A.

Hideo Sawada
National Aerospace Laboratory
Chofu, Tokyo, 182
JAPAN

Hans Schneider-Muntau
National High Magnetic Field Laboratory
Tallahassee, FL 32306-4005
U.S.A.

SYMPOSIUM COMMITTEE

Nelson J. Groom, Symposium Co-Chair
NASA Langley Research Center
Hampton, VA 23681-2199
U.S.A.

Brad Paden, Symposium Co-Chair
University of California at Santa Barbara
Santa Barbara, CA 93106
U.S.A.

Sandy Johnson, Administrative Chair
NASA Langley Research Center
Hampton, VA 23681-2199
U.S.A.

An international steering committee assisted in selecting and reviewing submitted abstracts and in structuring the symposium sessions. The steering committee consisted of the following people:

Colin P. Britcher, Chair
Old Dominion University
Dept. of Aerospace Engineering
Norfolk, VA 23529-0247

Isaiah Blankson
NASA Glenn Research Center
MS/5-9
21000 Brookpark Road
Cleveland, OH 44135

David Trumper
Massachusetts Institute of Technology
77 Massachusetts Avenue
Cambridge, MA 02139

Jim Downer
Foster-Miller, Inc.
350 Second Avenue
Waltham, MA 02154

Alexander Kuzin
Moscow Aviation Technology Institute
Petrovka 27
Moscow, K-31, 103737
RUSSIA

Justin Schwartz
National High Magnetic Field Laboratory
1800 E. Paul Dirac
Tallahassee, FL 32306-4005

Raoul Herzog
MECOS Traxler
Industriestr. 26, CH 8404
Winterthur
SWITZERLAND

Atsushi Nakajima
National Aerospace Laboratory
7-44-1 Jindaiji-Higashi-machi
Chofu, Tokyo, 182
JAPAN

Jim Lauffer
Sandia National Laboratories

P.O. Box 5800
Albuquerque, NM 87185-0557

The goal of the symposium was to examine the state of technology of all areas of magnetic suspension and to review recent developments in sensors, controls, superconducting magnet technology, and design/implementation practices. The symposium included 18 sessions in which a total of 53 papers were presented. The technical sessions covered the areas of bearings, controls, modeling, electromagnetic launch, magnetic suspension in wind tunnels, applications, flywheel energy storage, rotating machinery, vibration isolation, and maglev. A list of attendees begins on page xiii.

The first symposium in this series was organized by NASA Langley Research Center and held at Langley Research Center, Hampton, Virginia, on August 19-23, 1991. The proceedings of the first symposium are available as NASA Conference Publication NASA CP-3152, Parts 1 and 2. The second symposium in the series, also organized by NASA Langley Research Center, was held at The Westin Hotel in Seattle, Washington, on August 11-13, 1993. The proceedings of the second symposium are available as NASA Conference Publication NASA CP-3247, Parts 1 and 2. The third symposium, organized by NASA Langley Research Center and hosted by the National High Magnetic Field Laboratory was held at The Holiday Inn Capital Plaza in Tallahassee, Florida on December 13-15, 1995. The proceedings of the third symposium are available as NASA Conference Publication NASA CP-3336, Parts 1 and 2. The fourth symposium, organized by NASA Langley Research Center, the National Aerospace Laboratory, Japan, the National High Magnetic Field Laboratory, and hosted by the National Aerospace Laboratory was held at The Nagaragawa Convention Center in Gifu City, Japan on October 30-November 1, 1997. The proceedings of the fourth symposium are available as NASA Conference Publication NASA/CP-1998-207654.

NASA / CP-2000-210291 第5回 磁気浮上技術国際会議 (2000年)

POSSIBILITY OF EXISTENCE OF NON-LINEAR ELECTROMOTIVE FORCE (EMF)

Osamu Ide, Clean Energy Laboratory, Tokyo, Japan

ABSTRACT

It is well known that a conventional Faraday electromotive force (EMF) is proportional to the time derivative of the magnetic flux. The author made a prototype of a motor driven by the current discharged from the capacitor of an LC circuit and performed an investigation of its characteristics, experimentally and theoretically. The results – when motor drive units of a specific design are installed to drive the motor – confirm the phenomenon that unknown EMF components are created and that these can not be explained only with the conventional Faraday EMF model.

The unknown EMF is, for the most part, proportional to a function of the second-order time derivative of the magnetic flux applied. It is also evident that there is even a possibility of the existence of components that are dependent on the third-order, or higher, time derivatives of the magnetic flux applied. Furthermore, it must be noted that the direction of the EMF generated is always in the direction that accelerates the current flow discharged from the circuit.

INTRODUCTION

In a previous work[1,] it is reported that a motor driven by the current discharged from an LC resonance circuit, indicates the creation of an anomalous EMF when the magnetic fields generated from the coil units which are composed of such motor drive units are set to repel each other (repulsion mode), together with the fact that the EMF created is in the direction to accelerate or encourage the discharged current. The results obtained in previous work suggest the existence of a positive EMF that is substantially different in nature from the conventionally known back-EMF. In addition, the results of a theoretical analysis which was done based on a computer simulation also support the assumption that this positive EMF is the result of some anomalous phenomenon that is outside the range that can be explained by the conventional Faraday's law.

In this paper, further experimental and theoretical investigation was made of the results obtained in the previous study.

In the previous study, the positive EMF was observed only when the magnetic fields generated from each motor driver unit composed of a pair of the single-coil units are set to repel each other. (Repulsion mode). A double-coil unit, which is somewhat different from the single-coil ones previously used in the design, was also used for this research. In all other respects the prototype motors were identical.

The motor prototype used in both studies has two sets of drive units, each of which is installed on the stator of the motor. Each drive unit is composed of a pair of driving coils with coaxial alignment in a face-to-face configuration so the pair sandwiches the rotor along the horizontal plane of the motor axis.

The circuit controller operates the driving coils so the magnetic fields generated will be in the opposite direction.

Each of the double-coil units making up the drive unit used in this study is composed of two coils, an inner coil and an outer coil, being connected in series with each other and sharing a common center, and has a total of three paramagnetic core plates that are made of Permalloy 45. One of the core plates is set in the common center position of the coil unit, and the other two are set in the spaces between the inner and outer coils. The motor using the double-coil units displays the existence of a positive EMF of a significantly higher voltage compared with the EMF values obtained in the previous study. It is also possible that a slight repulsion force exists between the inner and outer coils of the double-coil unit.

On the other hand, the theoretical equations used for the computer simulation and theoretical analysis were projected to a higher level of precision than in the case of the previous study. In that work, the computer-simulation analysis was made on the supposition that the inductance of the coil varies in approximation depending upon the position of the cores according to a first-order algebraic equation. However, such a first-order approximation is effective only when the motor's rotation speed is in the low range. It is speculated that, as the motor's rotation speed increases, the obtained inductance value to be input to the simulation equation would greatly deviate from the corresponding experimental values.

In contrast to that, this study features that a third-order equation for the time derivative of magnetic inductance should be introduced to replace the simple first-order equation used in the previous study. The introduction of the new, improved equation allows the calculated inductance values to very closely match the corresponding measured values. This, in turn, enables the author to perform a computer simulation on EMF with a higher degree of precision. Consequently, the theoretical analysis by the computer simulation resulted in substantially more precise EMF values compared with those of the previous case study, which is based simply on Faraday's law in an unmodified form. The accuracy of the theoretical analysis based on the new approximation equation indicates an improvement of nearly a hundred-fold.

Computer-simulation analysis based on the new equation was made also on the result of the previous study that used a single-coil type. The degree of deviation was represented by the difference of the values that were obtained in the experiment from the theoretical values.

The deviation between the experimental and theoretical values and the time derivative for the inductance were used to evaluate the level of unknown EMF that was generated. A very interesting result was obtained after performing this evaluation.

In the previous study in which single coils were used, the unknown positive EMF was observed only when the magnetic fields generated from a motor drive unit were in repulsion mode. However, in this study, a positive EMF – although it was less intense – was observed even when the magnetic fields from a drive unit are set in attraction mode. Thus, when a drive unit using the double-coil units is in repulsion mode, the anomalous EMF will appear more conspicuously for easier observation. Based on the above, it is speculated that such phenomenon could occur in any type of electromagnetic system, (motor,generator,transformer etc.) as well as that it might be too weak to be detected because the intensity level of such components is much lower compared to that for conventional Faraday EMF.

The intensity level of the unknown EMF also varies depending on the time derivative of inductance, indicating an upward curve of a nonlinear nature. The fact that a certain amount of order is observed in the obtained deviation data means that the data obtained is a significant indication of the existence of the unknown factors.
In other words, there is a possibility that there could be additional non-linear components that have not yet come to the attention of the academic community. The conventional Faraday EMF is only indicative of the linear component.

DESCRIPTION OF THE MOTOR PROTOTYPE USED FOR THE RESEARCH

The basic electrical circuit of the motor drive unit of the motor prototype is shown in **Fig.1**. Two motor drive units are installed on the motor prototype system used for the experiment. The current discharged from capacitor **C**, whose initial voltage is $+V_0$, runs through the components composing the circuit. Each motor drive unit installed on the stators is made up of a pair of coil units (**L_1, L_2**).

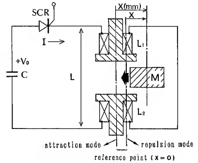

Fig. 1 The basic electrical circuit of a motor drive unit of the motor prototype

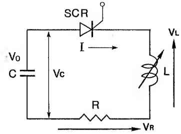

Fig. 2 The equivalent electrical circuit diagram of the motor prototype

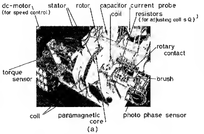

Fig. 3(a) A photograph of the whole view of the motor prototype system

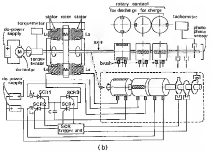

Fig. 3(b) An illustration of the configuration of the whole motor prototype system

A simplified circuit diagram that is equivalent to the circuit described above is shown in **Fig. 2.** The resultant value L of the inductance of L_1 and L_2 is intrinsically variable, because it is influenced by the position of core plates M on the rotor when the paramagnetic core plates are moved by the attraction force applied by the motor drive units.

A photograph and an illustration of the configuration of the whole the motor prototype system used for experiment is shown in **Fig. 3(a)** and **Fig. 3(b).** The system is an embodiment of the circuit diagram shown in **Fig. 1.** It is a motor that allows continuous operation. Core plates $\mathbf{M_1}$ and $\mathbf{M_2}$ made of a paramagnetic substance Permalloy45 are installed on the rotor disk. The rotor disk is started by driving an auxiliary DC drive motor. The rotation rate can be set to a desired value over a wide range by setting the attached speed controller, and the rate is indicated on the tachometer.

Each motor drive unit is composed of a pair of the coil units, (L_1, L_3)and(L_2, L_4). The magnetic fields that are generated from each drive unit can be set to either attraction mode (N-S, N-S) or repulsion mode (N-S, S-N).

A set of the rotary contact units installed on the axis of the rotor is used to switch the circuit for charging or discharging. It is set in series in the circuit of each mode. It is designed so that the **SCR** will become ON after the rotary contact units are set to ON; and so that the rotary contact circuit will become OFF after the SCR is set to OFF when the sign of the recharge voltage is reversed. In the result, the SCR is protected from malfunctioning.

Two motor drive units composing of four coil units are installed on the two stators of the motor. (Each coil unit has two coils.) The two paramagnetic cores $\mathbf{M_1}$ and $\mathbf{M_2}$ are installed at an interval of 180 degrees around the perimeter of the rotor disk which is installed between the two stators. See reference

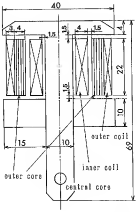

(a)

Fig. 4(a) A cross sectional view of the double-coil unit

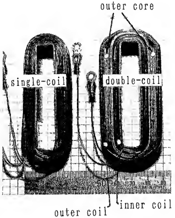

Fig. 4(b) Exterior views of a single-coil and a double-coil without their central cores

(1) for a detailed description on the positions of the coil units on the stator and of the paramagnetic cores on the rotor, since they are common to the previous study.

It is known that the values of the resultant inductance of the four coils L_1, L_2, L_3 and L_4, will reach a maximum when the paramagnetic cores on the rotor are at a certain angle. The angle is called "the Reference Point". There is a slight difference in the position of the reference points between attraction mode and repulsion mode (Fig.1).

In this research, two types of motor drive unit were examined to compare their performance, one using the newly developed double-coil units, and the other using the single-coil units tested in the previous research. A cross sectional view and a plan view of the double-coil unit, are shown in **Fig. 4(a)** and **Fig.4(b).**

The double-coil unit is composed of two coils, an inner coil and an outer coil. The magnetic fields generated from the two coils seem to repel each other, due to a design effect. It should be noted that two paramagnetic core plates of each double-coil unit are vertically installed in the spaces between the inner and outer coils. The core(s) of each coil are made of paramagnetic substance Permalloy 45 that is common to that of the rotor's cores .
The value Q of the double coil is intentionally set to a value equal to that of the single coil used in the previous research to check the effect of the newly-developed paramagnetic core plates inserted between the inner and outer coils. This means that the values of L and R of the two types of coil unit are approximately equal to the "discharge initiation point" which is described below.

EXPERIMENTAL METHOD

The relationship of the resultant inductance of all the coils existing to the position of the core plates, is shown in **Fig. 5.** Measurement of the inductance was done using a LCR meter. The values of the attraction force acting on the paramagnetic cores of the rotor were also measured so as to obtain the values to be used for reference.

From the curve to indicate the relationship between the resultant inductance (mH) and the relative position (mm) of the paramagnetic cores on the rotor's peripheral to the reference point, it can be seen that the resultant inductance of the coils gradually increases as the cores get closer to the coil units of the motor drive units under the influence of the attraction force applied. It is also known from the same curve that the value of the inductance will reach a maximum and that the torque acting on the rotor will become zero (gram meter) at the reference point (x = 0 mm). Incidentally, a back torque is generated if the core goes into a negative coordinate range by passing over the reference point.

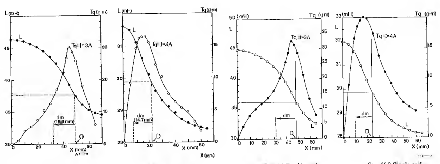

Fig. 5(a) Double coil (repulsion mode)

Fig. 5(b) Single coil (repulsion mode)

Fig. 5(c) Double coil (attraction mode)

Fig. 5(d) Single coil (attraction mode)

dm: Maximum displacement of the rotor in the period of T/2

Fig. 5 The relationship of the resultant inductance of all the coils existing, and of the torque Tq to act on the rotor, to the position of the core plates [the distance of the rotor from the reference point]

Discharge from the capacitor will be initiated when the paramagnetic core reaches a certain point in the distance D (mm) from the reference point. The distance D is called the "discharge initiation point". This point is located near the position where it is observed that the maximum torque acts on the rotor. The discharge initiation point had been set to a position where the paramagnetic cores will never pass over the reference point during the discharging period of a half cycle T/2, even when the rotor reach the maximum rotation speed required for the measurement. By taking such measures, it is impossible for the rotor to receive any back torque.

Fig. 6 shows that the waveforms to represent the continuous changes of the discharge current and the capacitor voltage when the motor is in operation.

(1) The capacitor is charged to a voltage $+V_0$ from the positive (+) terminal of a dc power source.

(2) When the rotor core gets close enough to the stator core to raise the voltage to the level of the discharge initiation point, SCR3 will be set to ON to initiate a discharge from the capacitor for the period of a half cycle (T/2). Subsequently the capacitor will be recharged to voltage -Vr.

(3) SCR2 is set to ON, and the capacitor is charged to voltage $-V_0$ from the negative (−) terminal of a dc power source

(4) SCR4 and subsequently SCR1 are set to ON, and the equivalent steps will be performed likewise in the discharging process in the opposite direction.

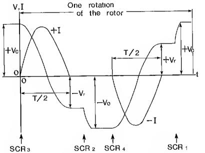

Fig. 6 The waveforms of the discharge current and voltage of the capacitor when the motor is in a continuous operation, with the action points of the SCRs

Thus the positive and negative discharging processes are repeated alternately in each cycle.

The absolute values of +Vr and -Vr corresponding to the desired rotation rate n (rpm) of the rotor, were measured experimentally. Each desired rotation rate was reached by starting from a standstill.

In order to minimize the effect of measurement errors, measurements were made 16 times for each rotation rate, namely, eight measurements for each of the positive and negative discharge processes. The average value of the 16 data sets was adopted as the measured value for each rotation rate.

The capacitance C of the capacitor used was 15.87 micro F, and the initial charge voltage V_0 was set to ±240 V. Measurement of the capacitor's voltage was done using a high impedance probe of 200 M ohms (dc - 15 kHz), and the intensity of the current was measured using a clamp-type probe. The waveforms to indicate the changes of the capacitor voltage and of the discharge current were continuously recorded using an oscilloscope with a digital memory. The measured data stored in the memory was then transmitted to a computer via a GP-IB mode line to be used as the input data for the theoretical analysis.

THEORETICAL ANALYSIS

A. The function of time on the inductance of the coil, to be derived from the approximation of the measured data

One of the major purposes of performing a theoretical analysis in this research is to derive a function for time from the inductance of the coil in the state that the rotor is moving. It is first necessary to derive a function for the position of the rotor (x) from the resultant inductance of the coil (L), based on the measured data.

Fig. 5 shows the measured data indicating the relationship of the inductance of the coil (L) to position of the rotor (x). Based on the data, an attempt was made to derive an equation simulating the (L - x) curve by means of theoretical analysis. In order to improve the level of precision, the assumption was made that L (mH) is a function of the 3rd order series of x (mm) for approximation (the equation (1)), instead of the straight line approximation (first order series) which was employed in the previous study.

$$L = A_0 + A_1 x + A_2 x^2 + A_3 x^3 \qquad \text{(mH)} \qquad (1)$$

Where, x (mm): position of the rotor

A_0, ... , A_3: Approximate values of the coefficients calculated from the measured values (L - x) (by the least squares method)

The relationship of the speed of rotation v to the position of the rotor x, is given by the equation (2). The relationship of the rotation speed v to the rotation rate n is given by (3), considering that the radius of the rotor is 1000 mm.

$$x = D - vt \qquad \text{(mm)} \qquad (2)$$

$$v = (1000 \times n) / 60 \qquad \text{(mm/s)} \qquad (3)$$

Where,

D (mm): Discharge initiation point to mean at distance D from the reference point

v (mm/s): Rotation speed of the rotor (rotor's peripheral speed)

t (s): Time elapsed after the discharge is initiated

NASA \ CP-2000-210291 第5回 磁気浮上技術国際会議 (2000年)

n (rpm): Rotation rate

The equation (4) of the inductance L as a function of time t, is derived from relationships (1), (2) and (3):

$$L = B_0 + B_1 t + B_2 t^2 + B_3 t^3 \quad [\mathrm{H}] \qquad (4)$$

Where,

$$B_0 = \left(A_0 + A_1 D + A_2 D^2 + A_3 D^3\right) \times 10^{-3}$$

$$B_1 = \left\{ \left(-A_1 - 2A_2 D - 3A_3 D^2\right) \times v \right\} \times 10^{-3}$$

$$B_2 = \left\{ \left(A_2 + 3A_3 D\right) \times v^2 \right\} \times 10^{-3}$$

$$B_3 = -A_3 v^3 \times 10^{-3}$$

The first order time derivative of the inductance (dL/dt) and the second order time derivative of the same are given by the relationships (5) and (6), respectively, being derived from the relation (4).

$$\frac{dL}{dt} = B_1 + 2B_2 t + 3B_3 t^2 \qquad (\mathrm{H/sec}) \qquad (5)$$

$$\frac{d^2 L}{dt^2} = 2B_2 + 6B_3 t \qquad (\mathrm{H/sec^2}) \qquad (6)$$

B. Equation to express the capacitor's voltage as a function of the elapsed time after discharge is initiated

The voltage V_L between the coil's two terminals (Fig. 2) is expressed by (7), which is derived from Faraday's law and relationships (4) and (5).

$$V_L = \frac{d\Phi}{dt} = \frac{d(Li)}{dt} = L\left(\frac{di}{dt}\right) + \left(\frac{dL}{dt}\right) i$$

$$= (B_0 + B_1 t + B_2 t^2 + B_3 t^3)\frac{di}{dt} + \left(B_1 + 2B_2 t + 3B_3 t^2\right) i \qquad (\mathrm{Volt}) \qquad (7)$$

Where, i (Ampere): Discharge current

The voltage between the capacitor's terminals Vc and the voltage between the terminals of the resistor composing of the circuit V_R, are given by (8) and (9), as functions of the capacitor C (Farad) and the discharge current i. (See Fig. 2).

$$V_c = \left(\frac{\int i dt}{C}\right) \qquad (\mathrm{Volt}) \qquad (8)$$

$$V_R = Ri \qquad (\mathrm{Volt}) \qquad (9)$$

The following relationship (10) is obtained based on Kirchhoff's law and relationships (7), (8) and (9).

$$V_c = V_L + V_R = \left(\frac{\int i dt}{C}\right)$$

$$= \left(B_0 + B_1 t + B_2 t^2 + B_3 t^3 \right)\frac{di}{dt} + \left(B_1 + 2B_2 t + 3B_3 t^2 + R\right) i \qquad (10)$$

METHOD OF EVALUATION

The unknown EMF (V_P) is expressed by (11), which is estimated from the recharged capacitor's voltage based on the assumption that an EMF other than Faraday's EMF exists.

V_P = [Measured value of Vr] – [Theoretical value of Vr] (11)

Where, Vr: capacitor's recycle voltage shown in Fig. 6

It is absolutely necessary to obtain the curve to express the relationship between the unknown EMF (V_P) and the inductance's time derivative to use it as the basis for evaluation of the EMF. In order to do so, it is necessary to take the following steps:

(a) Obtain the measured value of Vr corresponding to each rotation rate for experiment, first.

(b) Calculate the theoretical values of Vr corresponding to each rotation rate for experiment, by solving the equation (10) for Vc. The solutions of the equation are obtained by performing the following substeps (b1), (b2) and (b3):

(b1) Calculate the value of resistance loss R from the values of V_0 and Vr measured at n = 0, and from the integrated value of the square of the current $\int i^2 dt$ curve (current value) which had been obtained by measurement.

[by the equation(6) in the reference(1)]

(b2) Calculate the theoretical value of the capacitor's voltage Vc from the equation (10) using the Runge-Kutta method, while setting the initial conditions to t = 0, Vc = V_0 and i = 0, respectively.

(b3) Calculate the theoretical value of the recharged capacitor's voltage Vc to obtain the value of Vr at the time when the value i becomes zero again, after the discharge period for a half cycle is completed.

And calculate the value of Vp from the equation(11).

(c) Calculate the values of the first-order time derivative (dL/dt) and the second-order time derivatives (d^2L/dt^2) of the inductance for each rotation rate which is measured for experiment, at the moment when the discharge process is completed (t = T/2), from (5) and (6).

(d) Make graphs by plotting the values obtained in the above step (c) on the horizontal axis and the values V_P corresponding on the vertical axis. The graphs thus obtained are supposed to be the curves to represent the relationship of the unknown EMF to the inductance time derivatives of the first order and second order.

RESULTS

The results of the research are shown in **Fig. 7, Fig. 8** and **Fig. 9. Fig. 7** shows the curves indicating the dependency of the unknown EMF (V_P) upon the time derivative of the inductance (dL/dt). Both of the EMF curves obtained has a rising inclination of a non-linear nature, whether or not it is in attraction mode or repulsion mode, and regardless of whether it is a single-coil unit or a double-coil unit.

Fig. 8 and **Fig. 9** show the curves indicating the dependency of the unknown EMF (V_P) upon the second-order time derivative of the inductance of the coil (d^2L/dt^2). **Fig. 9** is an enlargement of the area near the origin of the x-axis shown in Fig. 8. Regardless of the conditions of the experiment, the curves obtained are rising curves of a non-linear nature, indicating patterns, which is significantly different from those shown in the **Fig.7.**

The results obtained indicate that the EMF value V_P always stays in the positive range and never becomes negative. The sizes of the absolute values of V_P obtained were in the following order based on the experimental factors; (a) > (b) > (c) > (d) [case (a) is the largest, (d) the smallest]. Here, (a) the double-coil unit in repulsion mode, (b) single-coil unit in repulsion mode, (c) double-coil unit in attraction mode, (d) single-coil unit in attraction mode.

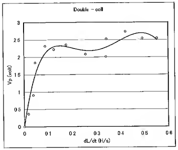

Fig. 7(a) Double coil (repulsion mode)

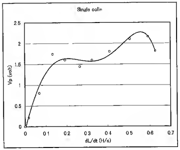

Fig. 7(b) Single coil (repulsion mode)

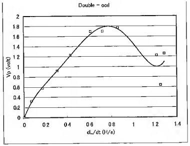

Fig. 7(c) Double coil (attraction mode)

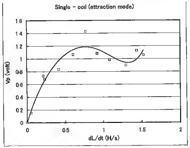

Fig. 7(d) Single coil (attraction mode)

Fig. 7 The dependency of the unknown EMF (V_P) upon the first-order time derivative of the inductance (dL/dt)

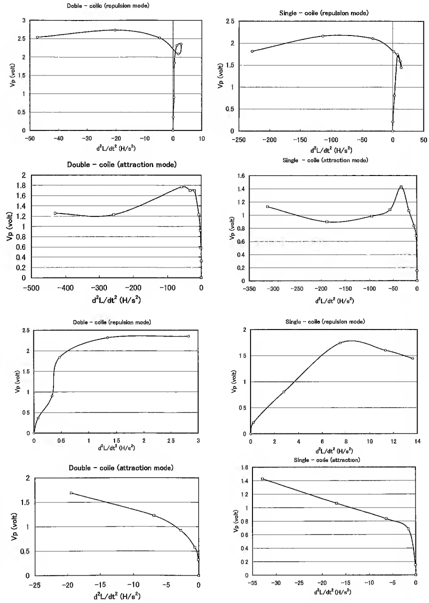

Fig. 9 An enlargement of the area near the origin of the x-axis shown in Fig. 8.

NASA / CP-2000-210291 第5回 磁気浮上技術国際会議 (2000年)

CONSIDERATIONS

There is a point that could be misunderstood with respect to this research. Let us consider an interpretation to introduce the possibility that the anomalous voltage (EMF) occurs because part of the kinetic energy of the rotor is converted into electrical energy. It is discussed in the following and proof is given that such an interpretation is wrong.

In order for the phenomenon of the above claim to occur, the rotor of the motor should rotate in the direction against the coil's attraction force during the capacitor's discharging process, under the conditions that an external force is being applied, while the system is in operation as a generator instead of a motor. However, it is obvious that the rotor can never be in such a condition under the circnmstances of this experimental system. Consequently, it was confirmed that the rotor never receives a repulsion force during the said discharge process of the capacitor, while it could receive an attraction force.

If the rotor's rotation rate is very high and the rotor passes the reference point during the half eycle capacitor discharge process, back torque will occur and cause the rotor to be decelerated. In such a situation it is possible that the author's claim could be refuted. But the experimental hardware used in this research was designed such that it never passed the reference point as long as the rotation rate stays below a certain level assumed for the measurements. The maximum rotation rate was set to 400 rpm. The maximum rate was set to a desired value by adjusting the discharge initiation point of each double coil. The above discussion should be enough to make this clear.

Another example of a common misinterpretation of the anomalous EMF observed is the hypothesis that the resistance loss of the coil had been decreased by a certain degree at higher speeds of rotation. Possible factors for this loss of coil resistance, such as copper losses (due to the skin effect), eddy current losses and hysteresis losses were considered and examined. It is known that these losses increase, as the frequency of the discharged current becomes higher. However, in the case of this experiment, it was discovered that the inductance of each coil increases due to the displacement of the coils during the discharge process, so that the frequency of the current will become slightly lower. Consequently, the coil's resistance loss could be reduced by a very small degree.

However, it is hard to regard this as the real cause of the anomalous EMF in question. The reason is that, if it is the cause, the largest value of the anomalous voltage EMF would be observed in the attraction mode of the motor drive unit using single coils, in which the highest increase in the rate of inductance was observed (**Fig. 5**). However, the experimental results shown in **Fig.** 7 and **Fig. 8** indicate an entirely opposite situation that the highest anomalous EMF is observed in the repulsion mode of the double coil, in which the lowest increase in the rate of inductance was observed. Therefore this hypothesis must also be turned down. Thus it is concluded that the only reasonable hypothesis remaining to effectively explain the anomalous phenomenon in question is to recognize the existence of an unknown EMF which is observed with the coils installed on each of the motor drive units of the motor. (Refer to (1))

Fundamentally, almost all aspects of this research are identical as those in the previous study described in reference (1) in terms of the experimental procedures and the experimental hardware system. The only difference in respect of the hardware system is the use of the motor drive unit composed of the newly-developed double coils, in addition to the case when the motor drive unit composed of the single coils was used. The results of the research under such conditions confirmed that a positive EMF had occurred whether the motor drive units were in attraction mode or repulsion mode.

In addition to the results obtained in the previous study, further characteristics of the EMF were uncovered after performing theoretical analysis based on a computer simulation of a higher level of precision. The resulting data from the simulation was compared to the experimentally measured values for the four categories of the experimental conditions.

Generally speaking, given the supposition that the conventional hypothesis is correct, it could be considered that the difference (V_P) of the measured value from the theoretical value, which is calcnlated from the simulation, is due to measurement errors or noise. In that case, it is customary that the sign of the deviation values of the measured values V_P from the corresponding theoretical values vary randomly, both in a positive and a negative direction.

However, the opposite conclusions were reached through the experiments performed in this research. Namely, value V_P is always positive and has a tendency to increase in a certain relationship with the rotation rate. This fact implies that certain physical factors that are unknown or cannot be explained as yet, are involved with the observed phenomenon.

With respect to the motor used in this experiment, it is possible to express its rotation rate in terms of the time derivative of the inductance of the coil (dL/dt). As is indicated in **Fig. 7**, the unknown EMF (V_P) is proportional to a non-linear function of dL/dt.

If it should be subject to Faraday's EMF law, V_P must be proportional to a linear function of dL/dt, according to Equation (7). On the other hand, if in the reality it is of a non-linear nature, it should have second and/or higher order time derivatives according to equation (12).

$$\frac{d^2\Phi}{dt^2}=\frac{d^2(Li)}{dt^2}=L\frac{d^2i}{dt^2}+2\frac{dL}{dt}\times\frac{di}{dt}+i\frac{d^2L}{dt^2} \qquad (12)$$

Furthermore, the measured values V_P versus the calculated second-order time derivatives of the inductance (d^2L/dt^2) are plotted in **Fig. 8 and Fig. 9**. The results show that all of the curves obtained have identical characteristics of an incremental tendency of a non-linear nature. Particularly in the case of attraction mode combined with the newly introduced double coils, beautiful curves were obtained from the mathematical standpoint, at any rate (**Fig. 9(c)**). This fact emphasizes that V_P is an unknown EMF having certain orderliness.

In addition, the fact that V_P is still in a non-linear relationship to the second order time derivatives of inductance d^2L/dt^2, implies that even higher time derivatives of inductance are involved with the phenomenon in question.

Postulating from the above, there is a possibility that the general form of the EMF is represented by an infinite series composed of the higher order time derivatives of magnctic flux, as shown by the equation (13).

$$EMF = K_0\Phi - K_1\frac{d\Phi}{dt} + K_2\frac{d^2\Phi}{dt^2} - K_3\frac{d^3\Phi}{dt^3} + \cdots\cdots + (-1)^n K_n\frac{d^n\Phi}{dt^n} + \cdots \quad (13)$$

In (13), the only terms which are already acknowledged, are the first term $K_0\Phi$ corresponding to the unipolar induction and the second term (K_1=1) corresponding to the Faraday EMF which is familiar to us in the aspect of power generation. The other 3rd, 4th, 5th... terms remaining, correspond to those of the unknown EMF which are discovered and discussed in this study.

What is important is *that the phenomenon to indicate an anomalous EMF is observed even with a coil which is in a magnetically unsaturated state*. It is suspected that the higher time derivative components of the non-linear terms of the EMF exist in any electromagnetic system that is in operation to some extent. However, in the past research of this field these components had been assumed to be measurement errors or noise.

When recalling the fact that EMF is a physical phenomenon of nature, it seems more reasonable to think in that way that EMF has characteristics of a non-linear nature, instead of purely linear ones.

CONCLUSIONS

Phenomena in a motor driven by oscillating current generated from a circuit composed of a capacitor and a coil were studied. It was observed that the capacitor's voltage was reversed to the opposite polarity by a half cycle after the start of the discharging process. The reversed voltage was used as the reference value to make comparisons of the experimental data with the theoretically estimated values obtained according to Faraday's law by computer simulation. Experiments were performed in four categories by changing between single coils or double coils and changing the motor drive units between attraction and repulsion modes (the directions of the magnetic fields).

Consequently, the following conclusions were confirmed:

1. The absolute values of the measured data always exceed the corresponding theoretical values obtained from the Faraday's law model in each of the four cases. This suggests that a positive EMF be always created in the motor.
2. A much stronger positive EMF is observed when the drive units are in repulsion mode compared to attraction mode.
3. The positive EMF observed experimentally can be represented in the form of a non-linear function of the time derivative of the inductance.

REFERENCES

1 *Osamu Ide*, "Increased voltage phenomenon in a resonance circuit of unconventional magnetic configuration", *J. Appl. Phys.*, Vol. 77, No. 11 (1 June 1995).

ACKNOWLEDGEMENTS

The author would like to acknowledge that this research was made with the strong support of the Natural Group Inc. The computer programs to generate simulations performing the theoretical analysis were prepared by Mr. Koji Mishima and Mr. Takashi Maeza. The illustrations and graphs for this paper were prepared by Mr. Toshiyuki Horii and Mr. Syunsuke Suzuki. Incidentally, the English translation of the whole text was prepared by Mr. Eiichi Yamamoto at Yama Trans Co. Ltd.

****